

## Strain-induced changes in the gate tunneling currents in *p*-channel metal–oxide–semiconductor field-effect transistors

X. Yang, J. Lim, G. Sun, K. Wu, T. Nishida, and S. E. Thompson<sup>a)</sup>

*Department of Electrical and Computer Engineering, University of Florida, Gainesville, Florida 32611*

(Received 9 September 2005; accepted 20 December 2005; published online 31 January 2006)

Changes in the direct gate tunneling current are measured for strained *p*-channel metal–oxide–semiconductor field-effect transistors (MOSFETs) on (100) wafers for uniaxial and biaxial stress. Decreases/increases in the gate tunneling current for various stresses primarily result from repopulation into a subband with a larger/smaller out-of-plane effective mass. Strain-induced changes in the valence band offset between Si and SiO<sub>2</sub> are also important but play a secondary role. Hole tunneling current is found to decrease for biaxial and uniaxial compressive stress and increase for biaxial tensile stress. The hole tunneling data is modeled using *k*·*p* self-consistent solution to Poisson and Schrödinger's equation, and a transfer matrix method. © 2006 American Institute of Physics. [DOI: 10.1063/1.2168671]

Strained silicon is being adopted into all high-performance nanoscale logic technologies.<sup>1–3</sup> The strain altered metal–oxide–semiconductor field-effect transistor (MOSFET) in-plane conductivity mass and its effect on mobility has been well studied.<sup>1–4</sup> Much less understood is how strain alters the out-of-plane conductivity effective mass and the valence band offset between Si and SiO<sub>2</sub>, both of which will affect the hole direct tunneling gate current, which dominates in ultrathin oxides. The SiO<sub>2</sub> to Si valence band offsets are altered by strain-induced (i) splitting of the four-fold degenerate heavy and light hole bands, (ii) shift in the electronic band by the volumetric change of the crystal and (iii) valence band warping which changes the out-of-plane mass and the subband energy in the quantum confined inversion layer. Changes in the out-of-plane mass directly affect the hole tunneling current by altering the tunneling probability and indirectly by shifting the subband energy<sup>4</sup> in the MOSFET inversion layer. It has recently been inferred from the hole mobility data that strain-induced band warping creates a small out-of-plane mass in the top band for biaxial tensile<sup>4</sup> and a large out-of-plane mass for uniaxial and biaxial compressive stress.<sup>3</sup> This strain-induced out-of-plane mass change should increase the hole tunneling current for biaxial tensile stress and decrease the current for biaxial and uniaxial compressive stress, which is what we observed.

For these reasons, it is important to understand how strain alters the MOSFET gate current. Recently, Zhao *et al.* measured the hole and electron gate current change versus tensile transverse stress on a (100) substrate, and the gate currents of the *n*-MOSFETs and *p*-MOSFETs were found to change linearly and in opposite directions as a function of uniaxial strain.<sup>5</sup> In this work, we experimentally measure the change in the hole tunneling current for more types of stress on (100) wafers, focusing on stresses commonly considered in the industry, i.e., biaxial and longitudinal uniaxial compression and tension.

Experiments were performed on industrial long channel 1 μm *p*-MOSFETs with *p*+ poly-Si gate electrodes, 10<sup>17</sup> cm<sup>-3</sup> *n*-type substrate doping, and 1.3 nm physical thickness nitrided SiO<sub>2</sub> gate insulators. Mechanical uniaxial

and biaxial stress is introduced into the MOSFET using four-point rods and concentric rings, respectively [Fig. 1(a)]. The MOSFET channel direction is ⟨110⟩. The change in gate current is measured at 1 V gate-to-source/drain/well bias at room temperature. The experimental data (dots) and physical model (lines) for the relative change in the gate tunneling currents versus various applied stresses are shown in Fig. 2. For *p*-MOSFETs, it is observed that gate tunneling current increases for biaxial tensile stress but decreases for biaxial and longitudinal compressive stresses.

We now quantify the strain-induced change in the gate tunneling current. We include strain-induced change in the Si subband energy level relative to the valence band of SiO<sub>2</sub>, valence band warping, and repopulation among the top three valence subbands. Stress-induced changes in the thickness of the gate insulator layer could also influence the tunneling current,<sup>6</sup> but it does not seem large enough to explain the experimental data or trends. For 300 MPa of mechanical stress, the Si channel strain and gate oxide strain is ~0.18%. Using a Young's modulus of 169 GPa for silicon and a Poisson ratio for oxide of 0.17, the oxide thickness change is only ~0.03%, which results in a leakage current change about 8% of what is observed in Fig. 2.

A qualitative schematic of the direct hole tunneling process for a *p*-MOSFET is shown in Fig. 1(b), where  $E_C$ ,  $E_V$ , and  $E_F$  are the silicon conduction band edge, valence band edge, and Fermi energy level, respectively.  $E_1$ ,  $E_2$ , and  $E_3$  are the energy levels of the top three subbands in the quantized inversion layer, resulting from the heavy, light, and split-off bands.  $V_{OX}=(\epsilon_{Si}/\epsilon_{OX})E_S \cdot T_{OX}$  is the oxide voltage drop, where  $\epsilon_{Si}$  and  $\epsilon_{OX}$  are the dielectric constants of silicon and silicon dioxide,  $E_S$  is the silicon surface electric field, and  $T_{OX}$  is the thickness of the oxide layer. As shown qualitatively in Fig. 1(b), the tunneling current in each *n*th band depends on the subband hole concentration, subband out-of-plane effective mass ( $m_{\perp,n}^*$ ), and tunneling barrier ( $\phi_{B,n}$ ).

The direct tunneling current density can be expressed as a sum of the tunneling current contributions of the *n* subbands,<sup>7</sup>

<sup>a)</sup>Electronic mail: Thompson@ece.ufl.edu

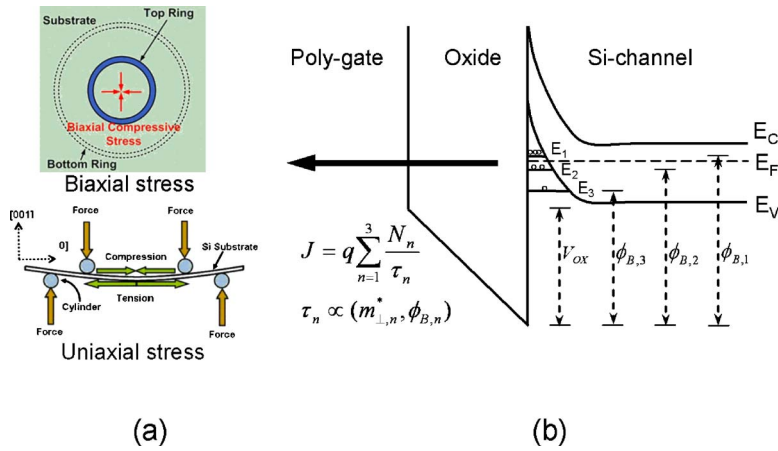


FIG. 1. (a) Wafer bending for biaxial and uniaxial stress; (b) schematic band diagram for direct hole tunneling in a *p*-MOSFET.

$$J = q \sum_n \frac{N_n}{\tau_n}, \quad (1)$$

where  $N_n$  is the subband inversion charge density,  $\tau_n$  is the corresponding lifetime of the subband, and  $q$  is the electronic charge. The charge density and subband energy levels are calculated by self-consistent solution of the one-dimensional Schrödinger and Poisson equation. For a MOSFET in the  $z$  direction, the electrostatic potential  $V_H(z)$  is determined by the total charge density from,<sup>4,8</sup>

$$-\frac{d^2}{dz^2} V_H(z) = \frac{q}{\epsilon_{Si}} [N(z) - n(z) + N_D(z)], \quad (2)$$

where  $N(z)$  is the mobile hole density,  $n(z)$  is the mobile electron density, and  $N_D(z)$  is the density of donors. Based on a six-band  $k \cdot p$  procedure,<sup>8</sup> we calculated the strain-induced band bending, charge density change, and out-of-plane effective mass. The lifetime of an  $n$ th subband state in the inversion layer is given by<sup>9</sup>

$$\frac{1}{\tau_n} = \frac{T_n(E_n)}{\int \sqrt{2m_{\perp,n}^*} [E_n - E_V] dz}, \quad (3)$$

where  $T_n$  is the hole transmission probability. By using the transfer matrix method, we obtained the transmission coefficient,<sup>10</sup>

$$T_n(E_n) = 1 - \left| \frac{m_{11} + m_{12} - m_{21} - m_{22}}{m_{12} + m_{21} - m_{11} - m_{22}} \right|^2, \quad (4)$$

where  $m_{11}$ ,  $m_{12}$ ,  $m_{21}$ , and  $m_{22}$  are simplified transfer matrix elements. The charge population of the lowest three subbands is calculated using

$$P_n(\sigma, E_S) = \frac{N_n(\sigma, E_S)}{N_1 + N_2 + N_3}, \quad (5)$$

where  $P_n$  is the population of the  $n$ th subband, and  $\sigma$  is the stress. The relative change of the leakage current can be expressed as

$$\frac{\Delta J}{J_0} = \frac{\Delta N_1 + \Delta N_2 + \Delta N_3}{N_1 + N_2 + N_3} + \frac{\Delta P_1/\tau_1 + \Delta P_2/\tau_2 + \Delta P_3/\tau_3}{P_1(0)/\tau_1 + P_2(0)/\tau_2 + P_3(0)/\tau_3}, \quad (6)$$

where  $P_n(0)$  is the population of the holes without stress,  $J_0$  is the leakage current without stress, and  $\Delta J = J - J_0$ . Since the total charge density is approximately constant with stress,  $\Delta N_1 + \Delta N_2 + \Delta N_3 = 0$ . The relative change of the leakage current can be simplified as

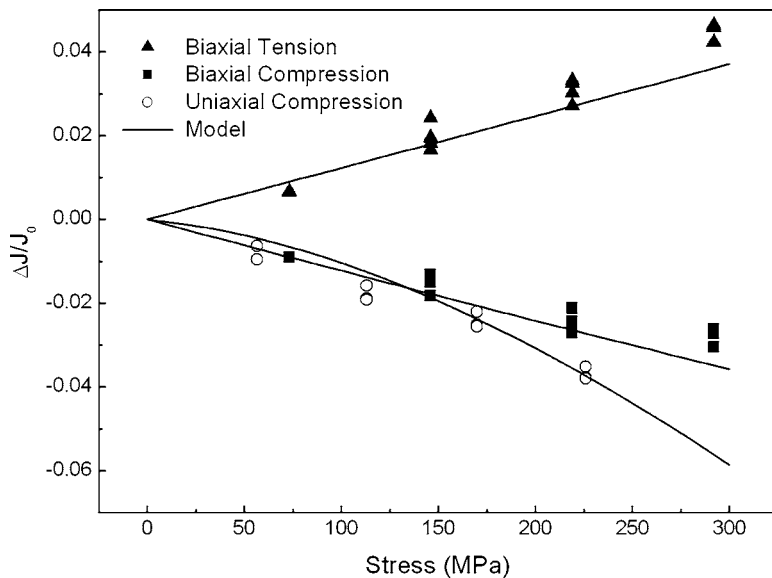


FIG. 2. The relative change of the tunneling currents versus applied uniaxial compression, biaxial compression, and biaxial tension, respectively. Dots are experimental data and lines are physical model.

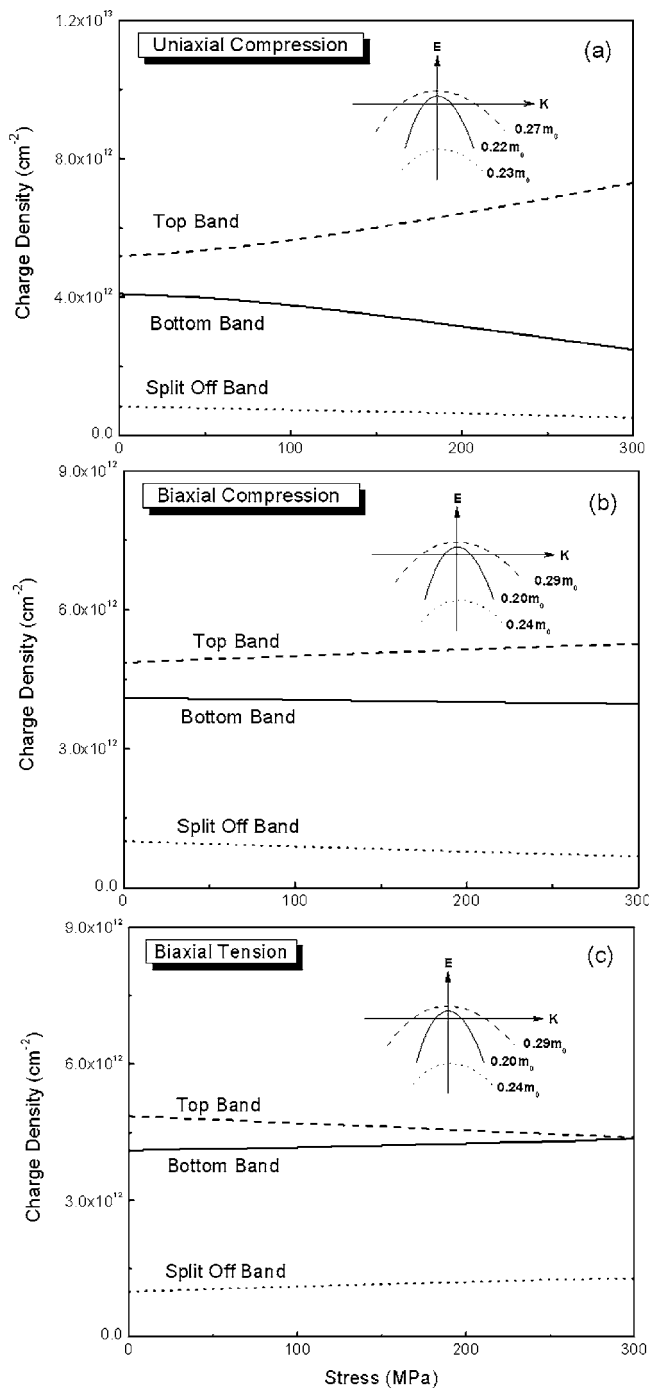


FIG. 3. Charge density versus applied stress for the top, bottom, and split-off bands for three applied stresses. (a) Uniaxial compression, (b) biaxial compression, and (c) biaxial tension. The inset shows the simplified hole valence band structure for the out-of-plane direction with the corresponding effective mass.

$$\frac{\Delta J}{J_0} = \frac{\Delta P_1/\tau_1 + \Delta P_2/\tau_2 + \Delta P_3/\tau_3}{P_1(0)/\tau_1 + P_2(0)/\tau_2 + P_3(0)/\tau_3}. \quad (7)$$

Figure 3 plots the charge density in the top three bands versus stress on the (100) wafer at 1 V gate bias. Also listed in Fig. 3 is the out-of-plane effective mass at the gamma point for the three highest subbands:  $0.29m_0$  ( $0.27m_0$ ),

$0.20m_0$  ( $0.22m_0$ ), and  $0.24m_0$  ( $0.23m_0$ ), respectively, for biaxial (uniaxial) stress on (100) wafers. The out-of-plane masses in the top three subbands are observed to be fairly constant at the  $\Gamma$  point for  $\sim 1$ –500 MPa of stress. The change in gate current from Eq. (7) is compared with the experimental data in Fig. 2, showing good agreement. Deformation potential  $a$  describes the shift in the energy levels while  $b$  and  $d$  the splitting. Values of  $a$ ,  $b$ , and  $d$  used are 2.46,<sup>11</sup>  $-2.58$ ,<sup>12</sup> and  $-14.3$ , respectively. The values chosen for  $a$  and  $b$  are commonly used<sup>13</sup> and similar values provide good fits to the strain-induced MOSFET threshold voltage shift.<sup>14</sup> The modeled results primarily depend on  $b$  and  $d$  and are only weakly affected by  $a$ . The value of  $d$  used in this work is larger than reported elsewhere<sup>13</sup> and is needed to fit the magnitude of the tunneling current decrease for compressive uniaxial stress ( $d$  has no effect on the modeled biaxial stress).

In summary, it is shown that a model based on subband repopulation can explain the (100) experimental  $p$ -MOSFET gate tunneling data. For stresses that produce favorable hole mobility versus electric field (biaxial and uniaxial compressive<sup>1</sup> as opposed to biaxial tensile<sup>4</sup> stress), it is observed that the gate tunneling current is reduced by stress, which results from the top subband having a larger out-of-plane effective mass. The same should be true for strain-induced electron mobility enhancement. “Good”  $n$ -MOSFET stresses such as biaxial and uniaxial longitudinal tensile stress decrease the direct electron tunneling current.<sup>5</sup>

The authors would like to thank the SRC, NSF (Grant No. ECS-0524316), and Air Force Office of Scientific Research (AFOSR), and Multi-disciplinary University Research Initiative (MURI) for funding this research.

<sup>1</sup>V. Chan, R. Rengarajan, N. Rovedo, W. Jin, T. Hook, P. Nguyen, J. Chen, E. Nowak, X. Chen, D. Lea, A. Chakravarti, V. Ku, S. Yang, A. Steegen, C. Baiocco, P. Shafer, H. Ng, S. Huang, and C. Wann, Tech. Dig. - Int. Electron Devices Meet. **2003**, 77.

<sup>2</sup>P. R. Chidambaram, B. A. Smith, L. H. Hall, H. Bu, S. Chakravarthi, Y. Kim, A. V. Samoilov, A. T. Kim, P. J. Jones, R. B. Irwin, M. J. Kim, A. L. P. Rotondaro, C. F. Machala, and D. T. Grider, *Proc. Symp. VLSI Technology*, 2004, p. 48.

<sup>3</sup>S. E. Thompson, M. Armstrong, C. Auth, S. Cea, R. Chau, G. Glass, T. Hoffman, J. Klaus, Ma Zhiyong, B. McIntyre, A. Murthy, B. Obradovic, L. Shifren, S. Sivakumar, S. Tyagi, T. Ghani, K. Mistry, M. Bohr, and Y. El-Mansy, *IEEE Electron Device Lett.* **25**, 191 (2004).

<sup>4</sup>M. V. Fischetti, Z. Ren, P. M. Solomon, M. Yang, and K. Rim, *J. Appl. Phys.* **94**, 1079 (2003).

<sup>5</sup>W. Zhao, A. Seabaugh, V. Adams, D. Jovanovic, and B. Winstead, *IEEE Electron Device Lett.* **26**, 410 (2005).

<sup>6</sup>K. Alam, S. Zaman, M. M. Chowdhury, M. R. Khan, and A. Haque, *J. Appl. Phys.* **92**, 937 (2002).

<sup>7</sup>Y. T. Hou, M. F. Li, Y. Jin, and W. H. Lai, *J. Appl. Phys.* **91**, 258 (2002).

<sup>8</sup>R. Oberhuber, G. Zandler, and P. Vogl, *Phys. Rev. B* **58**, 9941 (1998).

<sup>9</sup>F. Rana, S. Tiwari, and D. A. Buchanan, *Appl. Phys. Lett.* **69**, 1104 (1996).

<sup>10</sup>X. D. Yang, R. Z. Wang, Y. Guo, W. Yang, D. B. Yun, B. Wang, and H. Yan, *Phys. Rev. B* **70**, 115303 (2004).

<sup>11</sup>C. G. Van de Walle, *Phys. Rev. B* **39**, 1871 (1989).

<sup>12</sup>M. Cardona and E. H. Pollak, *Phys. Rev.* **142**, 530 (1966).

<sup>13</sup>M. V. Fischetti and S. E. Laux, *J. Appl. Phys.* **80**, 2234 (1996).

<sup>14</sup>J. Lim, S. E. Thompson, and J. G. Fossum, *IEEE Electron Device Lett.* **25**, 731 (2004).